# Towards Friction Potential Estimation for Motorcycles

Florian Klinger(✉), Christoph Ott, Agnes Poks, Johannes Edelmann, and Manfred Plöchl

Institute of Mechanics and Mechatronics, TU Wien, Austria
florian.klinger@tuwien.ac.at

**Abstract.** Estimation of the actual friction potential from measured vehicle states has been extensively explored for passenger cars, but lacks attention for motorcycles. Several aspects towards friction potential estimation for motorcycles are discussed in this study: (i) analysis of the characteristics of motorcycle tyres on different surfaces and conditions by using an instrumented motorcycle, (ii) analysis of the theoretical performance of an EKF-based friction potential estimation approach by means of simulation studies, and (iii) analysis of the feasibility of using a wetness sensor on the motorcycle to gain information on actual road conditions.

**Keywords:** Friction Potential Estimation · Extended Kalman Filter · EKF · Motorcycle · Tyre Characteristics · Road Conditions · Wetness Sensor

## 1 Introduction

The forces transmitted in the contact area of the tyres with the road are decisive for the handling dynamics and safety properties of road vehicles. Demanded forces that exceed the limits of friction may lead to a loss of stability, with potentially dangerous consequences, especially for motorcycle riders. Knowledge of the actual friction potential, however, may improve the performance of safety systems such as Anti-Lock Braking System (ABS), Traction Control System (TCS), and Stability Control System, and may also be helpful for the development of further Advanced Driver Assistance Systems (ADAS).

Methods for online estimation of the actual tyre–road friction potential can be basically classified into *cause-based* and *effect-based* [1]. The former methods are based on the detection of environmental (temperature, rain, etc.) or road surface conditions (water, ice, etc.). This can be done predictively within certain limits, but usually allows just for a classification of the actual friction potential. The latter methods rely on measurable effects of the current tyre–road contact conditions on the dynamic behaviour of vehicle and tyres. This allows for an estimation of the friction potential, but valid and yet sufficiently simple models of vehicle and tyres are required to adequately represent their behaviour at different friction conditions.


G. Mastinu et al. (Eds.): AVEC 2024, LNME, pp. 550–556, 2024.
https://doi.org/10.1007/978-3-031-70392-8_78

Various approaches for friction potential estimation are presented in vehicle dynamics literature, but refer almost exclusively to two-track vehicles, see e.g. [2–4]; an exception thereof is [5], wherein nonlinear regression methods are applied to estimate the friction potential during braking manoeuvres for a motorcycle. In this proceedings, selected aspects of an ongoing study towards friction potential estimation for motorcycles based on the magic formula (MF) tyre model and an extended Kalman Filter (EKF) approach are discussed, along with the first results from an analysis using a wetness sensor on a motorcycle.

## 2 Tyre Characteristics at Different Road Conditions

In a first step, the longitudinal characteristics of the front and rear tyres of an actual motorcycle have been analysed in order to identify applicable effects with regard to friction potential estimation. Starting from an available MF tyre parametrisation (from measurements on a flat track test rig), the scaling factors of the MF tyre model were adjusted to adapt the tyre characteristics to different surfaces and conditions found at the braking platform of the ZalaZONE proving ground in Hungary. Respective measurement data was collected by means of an instrumented motorcycle, and a procedure similar to [6] was employed to derive tyre forces and slip values at the front and rear tyres from coast down, constant speed, and acceleration and braking manoeuvres.

Figure 1 shows the resulting tyre characteristics of the front and rear tyres with the traction coefficient $\mu = F_x/F_z$ and the corresponding longitudinal slip $\kappa$. Comparing the orange and blue lines reveals a remarkable drop of the friction potential from dry asphalt to wet polished concrete, while the slope at small values of longitudinal slip κ remains unchanged. Note, that for the rear tyre, the friction potential is fully exploited

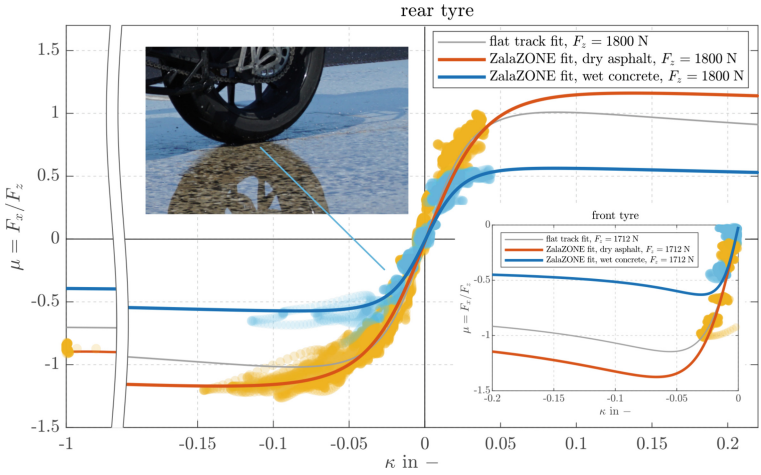


**Fig. 1.** Comparison of the longitudinal characteristics of the motorcycle tyres derived from measurements on a flat track test rig (grey) as well as from road tests with an instrumented motorcycle on dry asphalt (orange) and wet polished concrete (blue).

in wet conditions, while maximum tyre forces at higher positive slip values cannot be reached in dry conditions since a lift-off of the front tyre would occur (wheelie).

The same limitation applies to the front tyre under braking (stoppie). Besides, and due to the lack of driving forces, only negative slip values are used for the characterisation of the front tyre from on-road measurements. Yet, one may conclude that an effect-based friction potential estimation approach based on pure longitudinal excitation due to acceleration and braking, and relying on the diverging characteristics of the tyres in the (beginning of the) non-linear region seems promising.

## 3 Performance of EKF Based Friction Potential Estimation

It seems reasonable to investigate the performance of effect-based friction potential estimation approaches in idealised simulation studies first, before real-world measurements are taken into account. The former is addressed in this section, aiming to gain experience w.r.t. required excitation intensities for reliable estimation results, as well as related adaption time delays.

A discrete-time extended Kalman-Filter (EKF) according to [7] is implemented in Matlab. The selected structure of the algorithm is based on the planar three-dof motorcycle model depicted in the top left part of Fig. 2. In case of acceleration, the drive torque $T_2$ is the input to the estimator; longitudinal velocity $\hat{v}_x$, angular velocity $\hat{\omega}_2$ and friction potential $\hat{\mu}_{\max,2}$ comprise the estimated states of the EKF, which are updated at each time step by taking the chosen measurements in form of the longitudinal acceleration $a_x$ and the angular velocity $\omega_2$ of the rear wheel into account. Within the EKF, a simplified MF with $F_{x2} = F_{x2}\big(F_{z2}, \kappa_2, \mu_{\max,2}\big)$ is applied. The vertical tyre forces $F_{z1}$ and $F_{z2}$ required within the EKF are related via the c.g. coordinates $a$, $b$, and $h$ to the longitudinal acceleration $a_x$ from the previous time step. In the case of braking at the front wheel only, a corresponding approach is realised.

The model of Fig. 2 is used as simulation model with the full MF tyre model in longitudinal direction, and with overlayed white noise. For simplicity, the front and rear tyre characteristics are presumed to be equal, such that only one friction potential $\hat{\mu}_{\max}$ is estimated for both tyres by the EKF. Variations of the tyre–road friction potential are realised by altering the scaling factor $\lambda_{\mu x}$ of the MF tyre model. A synthetic, sawtooth-like torque profile was selected, with alternating drive and braking inputs $T_2 > 0$ and $T_1 < 0$ at the rear and front wheel, respectively, resulting in acceleration and braking sections for a duration of two seconds each. Several instantaneous changes of $\lambda_{\mu x}$ and thus $\mu_{\max}$ are included in the manoeuvre. The linear increase of torque during a sawtooth provokes increasing wheel slips, and the peaks of the torques were selected that the traction coefficients $\mu_1$ and $\mu_2$ reach a certain fraction of the friction potential $\mu_{\max}$ during each segment, which will be referred to as "excitation intensity" in the following. In the bottom plot in Fig. 2, the dashed lines show the traction coefficients $\mu_1$ and $\mu_2$ for the front and rear tyre, respectively, and the dash-dotted line indicates the excitation intensity, which is set here to approx. 80% of $\mu_{\max}$. In this form, the manoeuvre provides ideal conditions for testing the EKF by comprising persistent and high excitations while remaining within the wheelie and stoppie limitations.

The estimated friction potential $\hat{\mu}_{\max}$ converges in steps to the predefined $\mu_{\max}$ as can be observed by the blue line in the bottom plot of Fig. 2. It was found that the

traction coefficients need to exceed an excitation intensity of 0.6 for the algorithm to reliably converge. In Fig. 2, the related adaption time delays of the EKF are summarized as bar chart. The adaptation time delay is the time from the instantaneous change of $\lambda_{\mu x}$ until $\hat{\mu}_{\max}$ converges to a $\pm 10\%$ error range of $\mu_{\max}$. Adaption time delays of few seconds can be observed, and tend to increase with increasing downward-steps of the friction potential: for the steps towards $\lambda_{\mu x} = 0.4$, more than one sawtooth-excitation are required for the algorithm to converge. Adaption time delays w.r.t. the upward steps appear to be close to each other. This effect can be explained in the present case by the fact that the traction coefficients $\mu_1$ and $\mu_2$ quickly exceed the former $\mu_{\max}$ after an upward-step, which gives a clear sign to the EKF that $\mu_{\max}$ must have raised as well.

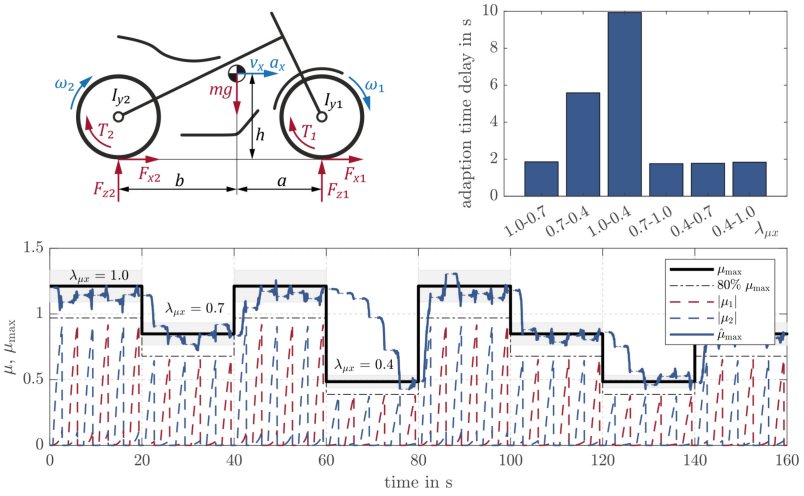


**Fig. 2.** Top left: three-dof motorcycle model for EKF and simulation. Bottom: simulated acceleration and braking manoeuvres with changing and estimated friction potential. Top right: adaption time required by the EKF to detect changes of the friction potential.

## 4 Analysis of Sensor-Based Detection of Wet Road Surfaces

To overcome limitations of the effect-based estimation method w.r.t. required excitation intensity and adaption time delays, the potential of a cause-based method to gain information on the actual road conditions is analysed in this section.

Multiple sensor principles for the purpose of detecting and quantifying road wetness are discussed in literature, see e.g. [8, 9], and recommendations for the positioning of such sensors at passenger cars are given based on different mechanisms of water spray ejection of rotating tyres.

In order to analyse the potential at motorcycles, two identical piezo-electric wetness sensors were applied to the instrumented motorcycle. First, a decision had to be made about the position of the sensors. Having in mind that the front tyre experiences changes in road conditions first, and already displaces some water from the road such that the

rear wheel experiences less road wetness when following the front wheel in the same track, it seems reasonable to place both sensors in the area of the front wheel. Two distinct positions have been selected, and are illustrated as orange rectangles in the top left sketch in Fig. 3: the first one is attached to the guard plate below the engine, such that the sensor is most directly hit by the water picked up by the tread of the front tyre; the second one is placed beneath the front fender, such that the sensor gets in contact with the spray circumferential to the front tyre. Impinging water droplets excite vibrations of the membrane of each sensor, resulting in oscillating analogous voltage output signals, which were recorded with a sampling rate of 50 kHz at the instrumented motorcycle.

Multiple measurements with different water heights on different surfaces have been conducted, with different velocities and different engine speeds. The recorded sensor signals were then analysed in both time and frequency domains, and from a comparison between the different mounting positions, the one beneath the front fender was found to be favourable. This may be due to the reasons described in [8, 9] that there is not enough water picked up by the front tyre to impinge on the first sensor at lower water heights, or the sensor position was too high above the road; another dominant reason is attributed to the engine noise, which is more dominant in the signal of the sensor at the engine plate than beneath the front fender.

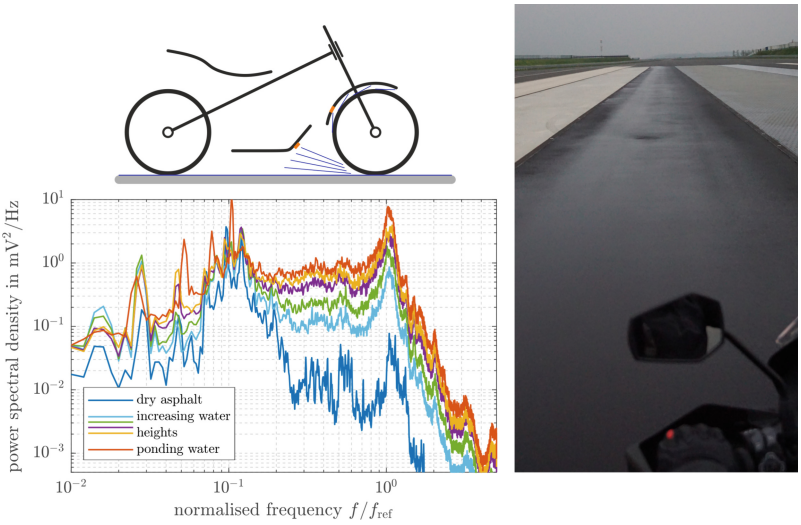


**Fig. 3.** Top left: selected positions of the wetness sensors at the motorcycle. Bottom left: power spectra for different water heights at an asphalt road resulting from the sensor mounted beneath the front fender. Right: asphalt road with different water heights at different tracks.

Power spectra of the signal of the sensor beneath the front fender are shown in the bottom left diagram in Fig. 3, resulting from different water heights on an asphalt road, which was traversed with a constant speed of 80 km/h in 4$^{\text{th}}$ gear. At lower frequencies, the sensor signal is influenced by engine noise, which possibly masks effects from impinging water. At higher frequencies above the sensor resonance frequency $f_{\text{ref}}$, the

spectra quickly decay with increasing frequency. The frequency range in between, however, allows for a clear distinction between dry asphalt (dark blue) and full wet asphalt with ponding water (dark orange), as well as between intermediate water heights at different tracks as depicted in the right picture in Fig. 3.

## 5 Summary

Analyses of the tyre characteristics of an actual motorcycle on different road surfaces and conditions reveal the possibility of effect-based friction estimation based on an extended Kalman Filter, relying on pure longitudinal driving and braking inputs. A performance analysis in a simulation environment confirms the feasibility in principle, but also shows that rather high excitation intensities and respective high longitudinal slip of the tyres are required, and that an estimation time of at least 2 s has to be accepted. As a possible solution, wetness sensors were investigated on the motorcycle. Encouraging results towards a quicker detection of wet road surfaces were found with a sensor positioned beneath the front fender of the motorcycle.

**Acknowledgements.** The measurement was carried out for R&D purposes at the ZalaZONE Automotive Proving Ground within the framework of scientific cooperation.

## References

1. Müller, S., Uchanski, M., Hedrick, K.: Estimation of the maximum tire-road friction coefficient. J. Dyn. Syst. Meas. Contr. **125**(4), 607–617 (2004)
2. Gustafsson, F.: Slip-based tire-road friction estimation. Automatica **33**(6), 1087–1099 (1997)
3. Tanelli, M., Piroddi, L., Savaresi, S.M.: Real-time identification of tire-road friction conditions. IET Control Theory Appl. **3**(7), 891–906 (2009)
4. Fichtinger, A., Edelmann, J., Plöchl, M., Höll, M.: Aquaplaning detection using effect-based methods. IEEE Veh. Technol. Mag. **16**(3), 20–28 (2021)
5. Savino, G., Baldanzini, N., Pierini, M.: Real-time estimation of road–tyre adherence for motorcycles. Veh. Syst. Dyn. **51**(12), 1839–1852 (2013)
6. Bartolozzi, M., Savino, G., Pierini, M.: Novel high-fidelity tyre model for motorcycles to be characterised by quasi-static manoeuvres. Veh. Sys. Dyn. **60**(12), 4290–4316 (2022)
7. Simon, D.: Optimal State Estimation. John Wiley & Sons, New Jersey (2006)
8. Schmiedel, B., Gauterin, F.: Unrau, H.-J.: Study of system layouts for road wetness quantification via tire spray. Autom. Engine Technol. **4**(1), 63–73 (2019)
9. Döring, J., Beering, A., Scholtyssek, J., Krieger, K.L.: Road surface wetness quantification using a capacitive sensor system. IEEE Access **9**, 145498–145512 (2021)